Revista Facultad de Ingeniería
ISSN: 0717-1072
facing@uta.cl
Universidad de Tarapacá
Chile

González P., Vicente; Segovia V., Daniel; Rajo I., Eva; Vázquez R., José Luis; Martín P., Carlos
Analysis of short circuited ring patch operated at TM01 mode
Revista Facultad de Ingeniería, vol. 13, núm. 2, 2005, pp. 21-30
Universidad de Tarapacá
Arica, Chile

Rev. Fac. Ing. - Univ. Tarapacá, vol. 13 Nº 2, 2005, pp. 21-30

ANALYSIS OF SHORT CIRCUITED RING PATCH OPERATED AT TM_{01} MODE

Vicente González P.[1] Daniel Segovia V.[2] Eva Rajo I.[2] José Luis Vázquez R.[2] Carlos Martín P.[2]

Recibido el 5 de noviembre de 2004, aceptado el 21 de junio de 2005

ABSTRACT

This paper presents a comprehensive study of the theory of the short circuited annular-ring patch based on the cavity model. An analytical expression for frequency, fields, radiation pattern, efficiency and input impedance based on this model is shown. Simulations and experimental results are given to show the resonant frequencies, illumination fields, radiation patterns and input impedances for the 0 and 1 modes. Furthermore, it provides a simple formulation to design this type of antennas.

Keywords: Patch antenna, cavity model, short circuited annular ring patch, input impedance.

RESUMEN

Este artículo muestra un estudio sencillo de la antena en anillo cortocircuitado en base al modelo de cavidad. Se han extraído y mostrado en base al modelo de cavidad expresiones sencillas para la frecuencia de trabajo, campos en el interior de la antena, diagramas de radiación, eficiencia e impedancia de entrada. Resultados experimentales y simulaciones de las frecuencias de resonancia, de los campos de iluminación, de los diagramas de radiación y de las impedancias son mostradas para el anillo en cortocircuito trabando en modo 0 y 1.

Palabras clave: Antena impresa, parche, modelo de cavidad, anillo cortocircuitado, impedancia de entrada.

INTRODUCTION

Among the various shapes of microstrip antennas, the rectangular and circular patches are the ones that have been more extensively studied [1], [4]. These patch antennas have a ring version that has been chosen as an alternative to the standard shape. These annular antennas are geometrically and electrically an intermediate step between printed loops and patches. Several interesting properties are associated with annular ring antennas. First of all, the size of the resonant ring is substantially smaller than that of the corresponding patch. Secondly, using annular topologies allows increasing the gain margin of the patch antenna in comparison with compact (circular or rectangular) ones.

A second alternative is the short circuited ring patch done by incorporating a shorting rod at the center of a circular patch; for this geometry, the resonant ring (TM_{11} mode) becomes greater than the original patch and, then, exhibits greater gain values. This makes margin of gain extend even more than the achievable with patches. The main drawback that this type of patch presents is that side lobes can be important when the size of the short circuited patch is big. Figure 1 shows a comparison between the different circular geometries and the margin of gains that can be obtained with each of them. This last property makes annular topologies particularly suitable for their integration in array antennas, allowing the optimum the optimum combined choice of the elementary radiator and the inter element spacing. From the theoretical point of view, ring patch antennas differ from traditional patch antennas by having an additional contour condition in the inner side of patch. This inner contour may be an open circuit or a short circuit. The open circuited annular patch antenna has been totally studied, so attention will be paid to the short circuited one. Figure 2 shows the geometry of a circular short circuited ring patch. The fundamental radiation mode in the open circuited patch antenna is the TM_{11} as in the corresponding circular patch. However there is an important difference when working with short circuited ring patches: the TM_{01} mode (the first index corresponds

[1] Instituto Tecnológico de Zacatecas México, aspirante al grado de doctor, depto. de Ingeniería Audiovisual y Comunicaciones, E.U.I.T. de Telecomunicación, Universidad Politécnica de Madrid - Campus Sur, Ctra. Valencia Km 7, E-28031, Madrid, España. vgonzalz@diac.upm.es.

[2] Depto. de Teoría de la Señal y Comunicaciones, Escuela Politécnica Superior, Universidad Carlos III de Madrid, Avda. Universidad 30, 28911 Leganés. Madrid, España.

to the azimuth variation) presents its resonance at much lower frequencies (depending on both radiuses) than in the circular and open ring patches, becoming the "fundamental" mode (lowest resonant frequency). This mode is often called Mode 0 and behaves slightly different from traditional circular patches since there is no cutoff frequency. It is evident that high order indexes in the radial variation have no sense from the practical point of view since they lead to bigger surfaces causing a strongly decreased efficiency. On the other hand, higher order modes in azimuth have been used, in practice, only for mobile applications. This means that almost all the practical patches work in the "dipolar" mode (TM_{01} for rectangular geometries and TM_{11} for circular ones). However, according to the above statements concerning the short circuited ring patch, two modes must be considered: Mode 0 (TM_{01}) that provides the lowest resonance frequency and mode 1 (TM_{11}) that behaves in a similar way to the corresponding mode in traditional circular patches.

Although the cavity model has been applied to study the short circuited annular-ring patch [5], [6], there are important omissions such as the field distribution is not analyzed and the 0 mode impedance is not considered at all (besides, values of directivity up to 12-14 dB are proposed which are impossible to reach in real patch antennas). A comprehensive study of the theory and the characteristics of the short circuited annular patch is given.

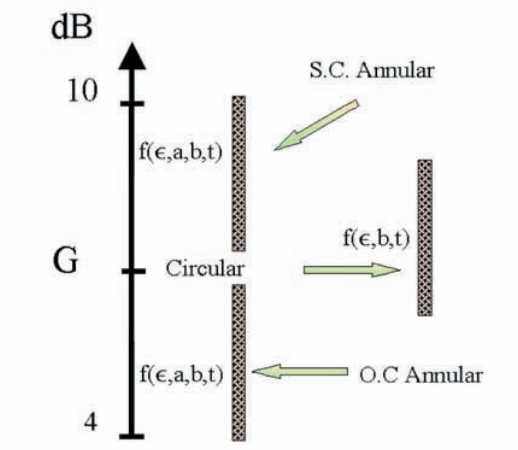

Fig. 1 Comparison between the different circular geometries.

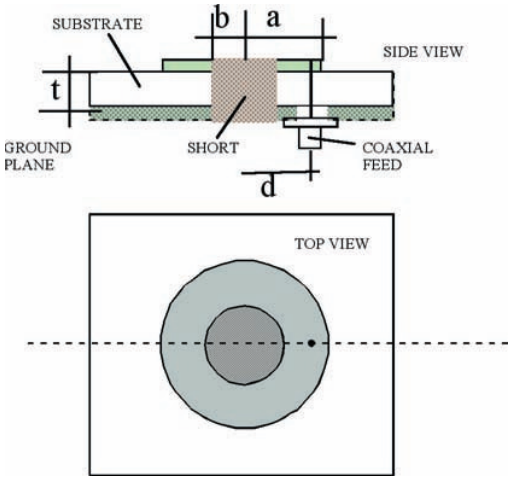

Fig. 2 Short Circuited Annular Ring Patch Antenna.

ANALYSIS OF THE SHORT CIRCUITED RING PATCH

A. Resonant frequencies

The geometry of the short circuited annular ring patch is shown in Figure 2. It has an outer radius *a*, an inner radius *b*, and is printed on the top of a substrate of thickness *t*. The model in the figure is fed through a coaxial probe located at a distance *d* from the center of the patch.

In the simple cavity model, the region between the patch and the ground plane is considered as a cavity bounded by electric walls on the top, bottom and inner edge, and a magnetic wall along the outer edge. If it is assumed that there is only TM modes propagating in the cavity, the resonant frequencies are determined by equation 1. It has also been assumed that the field distribution under the patch does not vary with the thickness of the patch (*t*) since $t<<\lambda$.

$$f_{mn} = \frac{k_{mn}}{2\pi a \cdot \sqrt{\mu_o \cdot \varepsilon}} = \frac{k_{mn} \cdot c}{2\pi a \cdot \sqrt{\varepsilon_r}} \qquad (1)$$

where the sub indexes mn represent the corresponding TM mode, *e* is the permittivity of the substrate, μ_0 is the vacuum permeability, *c* is the light velocity, ε_r is the substrate relative permittivity and $k_{mn,}$ are the roots of the following characteristic equation (2).

$$J_m'(k_{mn})N_m(k_{mn}c) - J_m(k_{mn})N_m'(k_{mn}c) = 0 \qquad (2)$$

Equation 2 comes from the boundary conditions in a ring cavity (electric wall for the inner edge and magnetic wall for the outer one); c is the ratio b/a, $J_m(x)$ and $N_m(x)$ are the first and second kind m^{th} order Bessel functions and the prime denotes the first derivative. Figure 3 shows the roots of equation 2 for different ratios b/a; it can be seen that the n^{th} subindex of the corresponding TM_{mn} mode has been fixed to 1 while the m^{th} one is varied from 0 to 4 (modes will be generally denoted according to the m^{th} subindex). It must be emphasized that the lowest resonance frequency is the corresponding to the 0 mode.

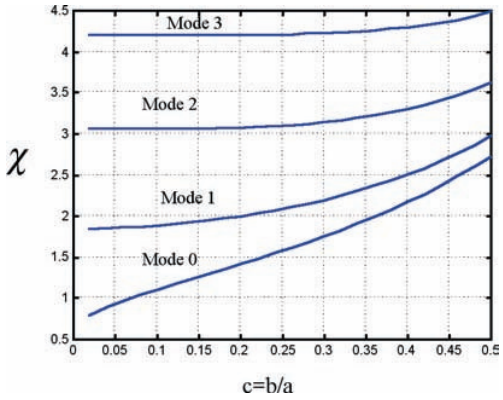

Fig. 3 Values of Roots of equation 2 for the short circuited Ring Patch.

A correction on the value of the outer radius, *a,* has been proposed as a technique to find out the value of the resonance frequency. Some authors [7] consider a suitable approach to model the antenna as a circular microstrip patch with radius $r=a-b$. This approach behaves well for higher modes but, only in a small variation margin of c, for lower ones. Schneider [8] has proposed to use an effective permittivity to take into account the effects of the fringing fields. Moreover a modification in the outer radius has also been suggested in [2], [8] resulting in the following empirical formula (3).

$$a' = a + (3/4)\cdot t \qquad (3)$$

This expression can be considered as correct in most cases.

B. Cavity fields

For the coaxial feeding case, the electromagnetic field excitation is due to a density current defined as

$$\vec{J} = I(\phi - \phi_o)\frac{\cdot\delta(r-d)}{d}\hat{z} \qquad (4)$$

Where d and Φ_0 denote the position of the feeding coaxial probe.

The fields within the cavity corresponding to the TM_{mn} mode are given by:

$$E_z^{mn} = A_{mn}\Big[J_m(k_0\sqrt{\varepsilon_r}r)N_m(k_0\sqrt{\varepsilon_r}b) + -J_m(k_0\sqrt{\varepsilon_r}b)N_m\Big]\cdot\cos m\phi$$

$$H_\Phi^{mn} = -\frac{j}{\omega\mu}A_{mn}\Big[J'_m(k_0\sqrt{\varepsilon_r}r)N_m(k_0\sqrt{\varepsilon_r}b) + -J_m(k_0\sqrt{\varepsilon_r}b)N'_m(k_0\sqrt{\varepsilon_r}r\Big]\cdot\cos m\phi$$

$$H_r^{mn} = -\frac{j}{\omega\mu}\frac{m}{r}A_{mn}\Big[J_m(k_0\sqrt{\varepsilon_r}r)N_m(k_0\sqrt{\varepsilon_r}b) + -J_m(k_0\sqrt{\varepsilon_r}b)N_m(k_0\sqrt{\varepsilon_r}r)\Big]\cdot\sin m\phi \qquad (5)$$

where A_{mn} is a constant depending on the corresponding *mn* mode and ϕ, r and z are the coordinates in a cylindrical system. When the patch is excited, for a general situation, several modes can appear. Then, the fields can be expressed as:

$$E_z^{mn} = j\omega\mu I\sum_{n=1}^{\infty}\sum_{m=0}^{\infty}\Big[R_{mn}\Big[J_m(k_0\sqrt{\varepsilon_r}r)N_m(k_0\sqrt{\varepsilon_r}b) - J_m(k_0\sqrt{\varepsilon_r}b)N_m(k_0\sqrt{\varepsilon_r}r)\Big]\cdot\cos m\phi\Big]$$

$$H_\Phi^{mn} = I\sum_{n=1}^{\infty}\sum_{m=0}^{\infty}\Big[R_{mn}\Big[J_m'(k_0\sqrt{\varepsilon_r}r)N_m(k_0\sqrt{\varepsilon_r}b) - J_m(k_0\sqrt{\varepsilon_r}b)N_m'(k_0\sqrt{\varepsilon_r}r)\Big]\cdot\cos m\phi\Big]$$

$$H_r^{mn} = \frac{I}{r}\sum_{n=1}^{\infty}\sum_{m=0}^{\infty}m\cdot\Big[R_{mn}\Big[J_m(k_0\sqrt{\varepsilon_r}r)N_m(k_0\sqrt{\varepsilon_r}b) - J_m(k_0\sqrt{\varepsilon_r}b)N_m(k_0\sqrt{\varepsilon_r}r)\Big]\cdot\sin m\phi\Big] \qquad (6)$$

Where R_{mn} is the amplitude of each mode present in the patch and is related to the corresponding A_{mn} and to the amount of energy associated to each propagating mode. Where w is the diameter of the probe that provides a uniform current [8]. Although equation 6 relates to a double infinite series, in most practical cases it converges very fast for m,n values lower than 5. Figures 4 and 5 represent the electrical fields inside the cavity as a function of the radius and the azimuthal angle. Figure 6 represents the current line distribution and 3D Ez field in the short circuited ring patch for the modes 0 and 1.

$$R_{mn} = \begin{cases} \dfrac{\pi w k_0^{\,2} \varepsilon_r \left[J_0(k_{0n}d) N_0(k_{0n}b) - J_0(k_{0n}b) N_0(k_{0n}d) \right]}{\left[\left(k_0 \sqrt{\varepsilon_r} \right)^2 - k_{0n}^{\,2} \right] \cdot \left[\dfrac{J_0(k_{0n}b)}{J_0(k_{0n}a)} - 1 \right]} ; m = 0 \\ \dfrac{\pi k_0^{\,2} \varepsilon_r \sin mw \cos m\pi \left[J_m(k_{mn}d) N_0(k_{mn}b) - J_m(k_{mn}b) N_m(k_{mn}d) \right]}{m \cdot \left[\left(k_0 \sqrt{\varepsilon_r} \right)^2 - k_{0n}^{\,2} \right] \cdot \left[\dfrac{J_m(k_{mn}b)}{J_m(k_{mn}a)} \cdot \left(1 - \dfrac{m^2}{\pi k_0^{\,2} \varepsilon_r a^2} \right) - \left(1 - \dfrac{m^2}{\pi k_0^{\,2} \varepsilon_r b^2} \right) \right]} ; \forall m \neq 0 \end{cases} \quad (7)$$

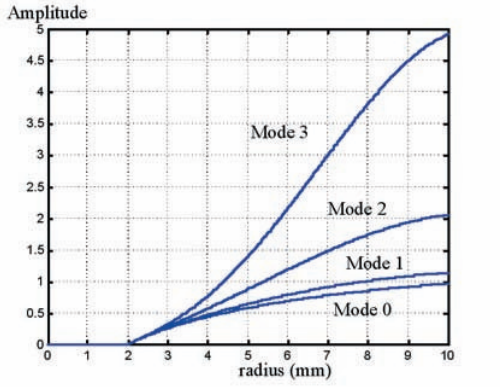

Fig. 4 Ez field versus radius of the patch.

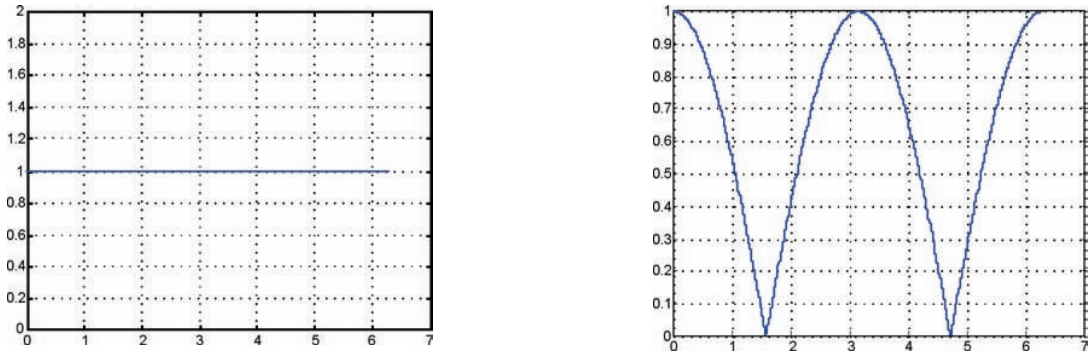

Mode 1 Mode 2

Fig. 5.1 Ez versus azimuthal angle in radians.

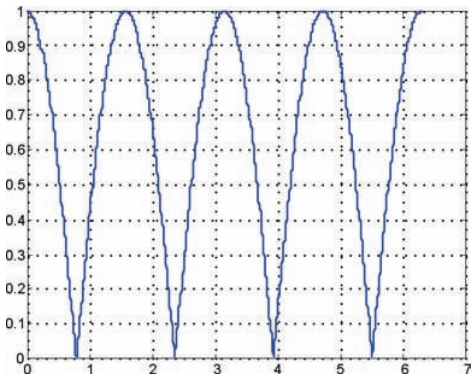

Mode 2

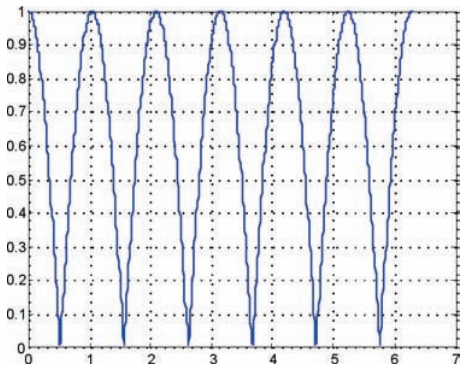

Mode 3

Fig. 5.2 Ez versus azimuthal angle in radians.

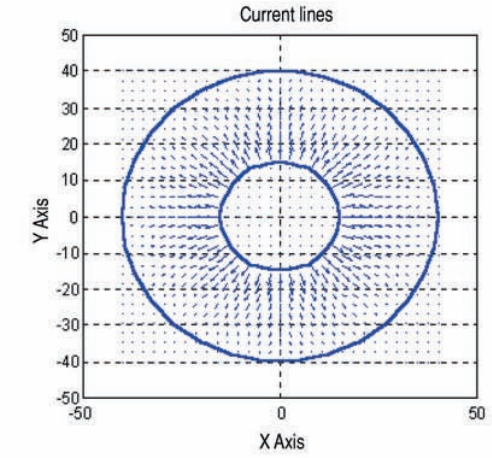

Mode 0

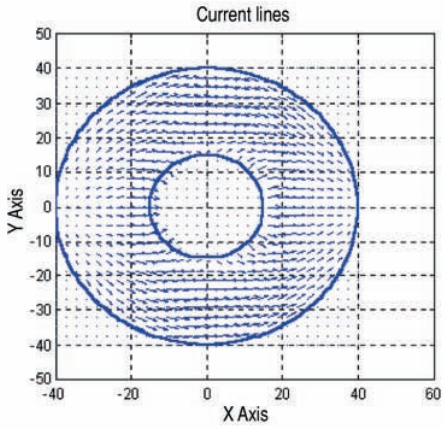

Mode 1

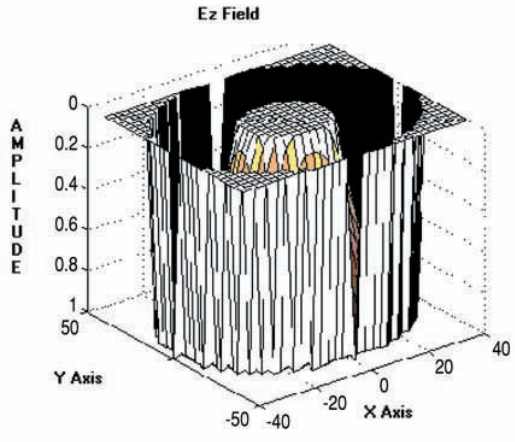

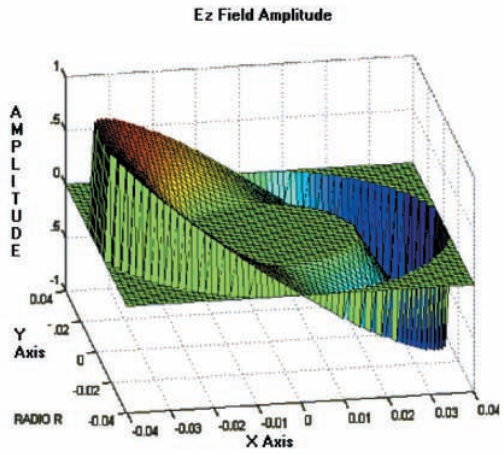

Fig. 6 Current line distribution in the patch (upper side) and 3D Ez Field for modes 0 and 1 side.

C. Input Impedance

The input impedance allows the definition of the antenna operation bandwidth and the analysis of the possibility of adding resonance to increase its bandwidth.

Although the input impedance of the shorted annular ring patch has not been calculated yet by using the cavity model, the method of calculation is well established [1], [2]. It involves the introduction of an effective loss tangent to take into account for the various losses in the cavity, namely the radiation, the dielectric, the conductor and the surface wave losses. The last quantity is quite small and can usually be neglected, for the case where the ratio between the substrate thickness and the wavelength (h/λ) be lower than 0.05 (e.g.). However, real patches have limited substrate and ground plane; then, when the surface wave reaches these edges, it transforms into a volume wave without decreasing the antenna efficiency although distorting (even strongly) the radiation pattern.

Then, the input impedance can be formulated as [1], [9] and [10], see (8).

The first term in brackets represents the contribution from the 0 mode while the double sum represents the contribution from all other modes, k_{eff} is the effective wave number which is given as:

$$k_{eff} = k_0\sqrt{\varepsilon_e(1 - j\delta_{eff})} \tag{9}$$

where δ_{eff} is the effective loss tangent given by [10]:

$$\delta_{eff} = \tan\delta + \frac{1}{t\sqrt{\sigma\mu\pi f}} + \frac{2\omega\cdot\mu\cdot t\cdot M}{\eta_0\cdot\varepsilon_r\cdot\left[\frac{J_m\left(k_{mn}\cdot a\right)}{J_m\left(k_{mn}\cdot b\right)}\cdot\left(1-\frac{m^2}{k_{mn}^2\cdot b^2}\right)-\left(1-\frac{m^2}{k_{mn}^2\cdot a^2}\right)\right]} \tag{10}$$

The quantity M is the following integral: see (11).

Note that the first term in the previous integral is zero for the 0 mode. Besides the double sum in (8) mainly affects to the upper modes so for the analysis of the TM_{01} or TM_{11} modes they must be discarded. It must also be noted that the mode 0 presents, in the same way as any other mode, an equivalent resonant RLC circuit. However, for low frequencies this mode behaves as a short circuit; for that reason it can be thought that at these frequencies another RC circuit looms. This RC circuit is composed of a resistor (with a very low value depending on the frequency) paralleled with a capacitor whose effect is negligible at the corresponding resonant frequency of the TM_{01}. This last effect at very low frequencies (quasi static) can be included in the overall equivalent circuit of the TM_{01} mode what would result in a double series resonant circuit (an RC circuit for low frequencies and the traditional RLC circuit for the corresponding resonant frequency of the TM_{01} mode). Although it could be thought of having a dual resonant antenna for the TM_{01} mode by tuning the RC circuit with an appropriate inductive coaxial probe, this is not so since the radiation properties of the lower frequencies are very poor.

$$Z_{IN} = R + jX = j\omega\mu\left\{\sum_{n=1}^{\infty}\frac{(J_0(k_{0n}t)N_0(k_{0n}b)-J_0(k_{0n}b)N_0(k_{0n}t))^2}{4(k_{eff}^2-k_{0n}^2)\left[\frac{J_0^2(k_{0n}b)}{J_0^2(k_{0n}a)}-1\right]}\pi k_{0n}^2+\sum_{m=1}^{\infty}\sum_{n=1}^{\infty}\frac{\left(\frac{\sin(mw)}{mw}\right)^2\left[N_m(k_{mn}a)J_m(k_{mn}t)-J_m(k_{mn}a)N_m(k_{mn}d)\right]^2}{\frac{2(k_{eff}^2-k_{mn}^2)}{\pi k_{mn}^2}\left[\frac{J_m(k_{mn}a)}{J_m(k_{mn}b)}\left(1-\frac{m^2}{k_{mn}^2b^2}\right)-\left(1-\frac{m^2}{k_{mn}^2a^2}\right)\right]}\right\} \tag{8}$$

$$M = \int_0^{\pi}\frac{m^2\cdot\cos^2\theta}{k_0^2\cdot\sin\theta}\cdot\left\{\frac{J_m\left(k_o\cdot b\cdot\sin\theta\right)}{b}-\frac{J_m\left(k_o\cdot a\cdot\sin\theta\right)}{a}\cdot\frac{J_m\left(k_{mn}\cdot b\right)^2}{J_m\left(k_{mn}\cdot a\right)^2}\right\}^2 d\theta + \int_0^{\pi}\sin\theta\cdot\left\{J_m\left(k_o\cdot b\cdot\sin\theta\right)-J_m\left(k_o\cdot a\cdot\sin\theta\right)\cdot\frac{J_m\left(k_{mn}\cdot b\right)}{J_m\left(k_{mn}\cdot a\right)}\right\}^2 d\theta \tag{11}$$

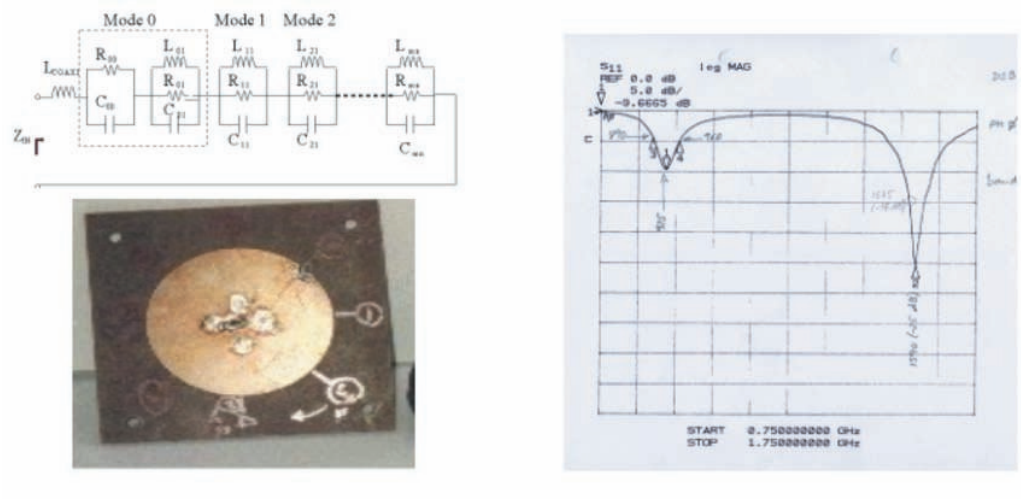

Fig. 7 Impedance model and prototype measured (left) with two resonances (right).

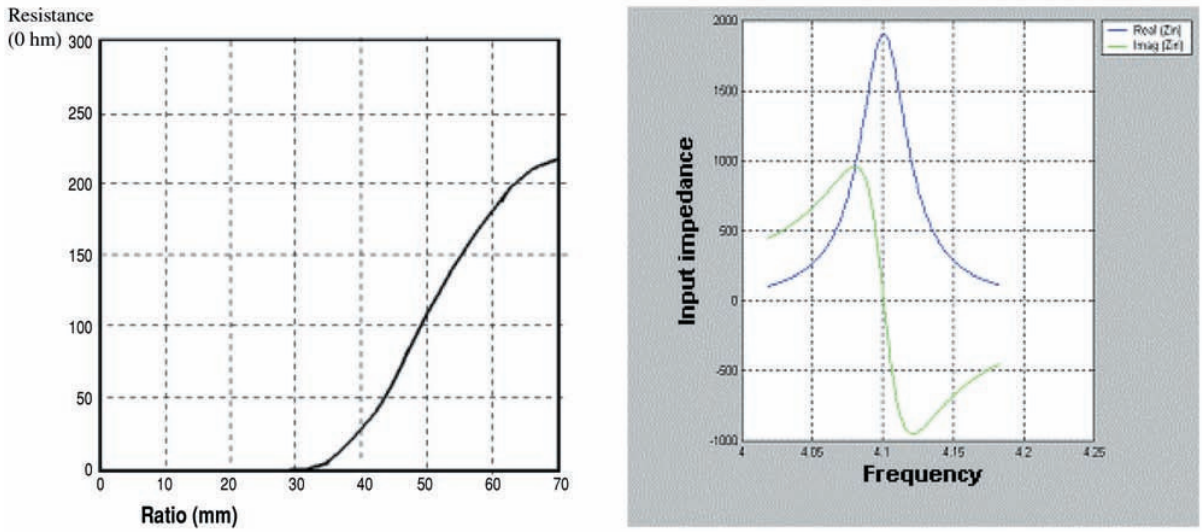

Fig. 8 Impedance vs radii (left) and Impedance vs frequency (right) in the mode 0.

According to the previous comments the complete equivalent circuit for the short circuited patch antenna is shown in figure 7. Figure 7 shows the two frequencies resonance and sc ring measured. The values for any element in the equivalent circuit are given as a function of the corresponding modes. By using previous equations, the input impedances for different modes can be easily plotted. Then figure 8 shows the input impedance for mode 0 as a function of the outer radius or frequency.

D. Radiated Fields

Once the internal fields and input impedance in the cavity have been determined, the radiated fields of a short circuited ring patch can be obtained either from the magnetic current approach on the fictitious magnetic wall in the outer region or the electric current distribution on the surface of the ring.

$$E_\theta = j^{m+1} A \frac{e^{-jk_0 r}}{r}\left[(J_m(k_{mn}a)N_m(k_{mn}b) - J_m(k_{mn}b)N_m(k_{mn}a)\right]J_m^{'}(k_0 b sen\theta)\cos m\phi$$

$$E_\phi = -j^{m+1} mA \frac{e^{-jk_0 r}}{r}\left[J_m(k_{mn}a)N_m(k_{mn}b) - J_m(k_{mn}b)N_{\boldsymbol{m}}(k_{mn}a)\right]\frac{J_m(k_0 a sen\theta)}{k_0 a sen\theta}\frac{\cos\theta}{sen\theta}senm\phi \quad (12)$$

where:

$$A = \frac{2tk_0 E_{mn}}{\pi k_{mn}}$$

The previous expressions represent the radiated field by only one mode without considering the effect of the probe. Mode 0 or 1 will be chosen according to the application required. The other modes are less interesting because of their smaller bandwidths and polylobed radiation patterns. Figures 9 and 10 show the radiation patterns simulated and measured for 0 and 1 modes.

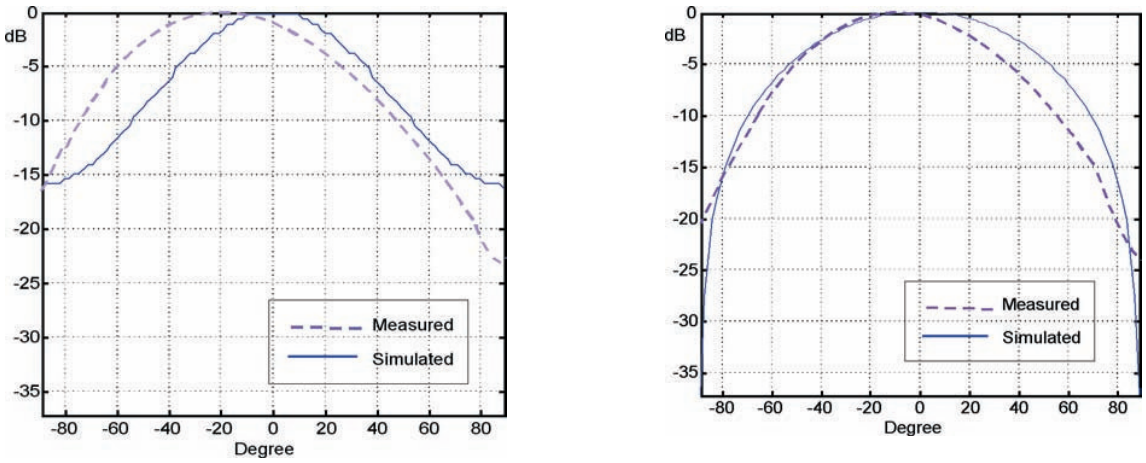

Fig. 9 Simulated and Measured radiation pattern in E (left) and H (right) plane (Mode 1).

The fundamental mode in the short circuited ring antenna is the mode 0 that has the characteristic of having a null in the zenith and a maximum in the azimuthal direction. For the same radiation mode, the radiation pattern is similar to that of a circular patch, although this antenna presents a better performance than the one using a circular geometry. It can be emphasized that this structure has a bigger gain. The directivity and gain can be given [1], [9] as: see (13).

$$D = \frac{4\pi}{\Omega_A} = \frac{4}{M\varepsilon_m} \quad (13)$$

M is the integral shown in 11. The gain is

$$G = \eta \cdot D \quad (14)$$

where the efficiency is given approximately [10]: see (15).

$$\eta = \frac{\frac{k_0^2 t}{\eta_0 k_{mn}^2 I}}{\frac{k_0^2 t}{\eta_0 k_{mn}^2 I_2} + \left[\frac{J_m^2(k_{mn}a)}{J_m^2(k_{mn}b)}\left(1 - \frac{m^2}{k_{mn}^2 b^2}\right) - \left(1 - \frac{m^2}{k_{mn}^2 a^2}\right)\right]\left[\frac{R_s}{\pi\omega^3\mu_0^2} + \frac{\varepsilon t\delta}{2\pi k_{mn}^2}\right]} \quad (15)$$

Where R_S is the surface resistance.

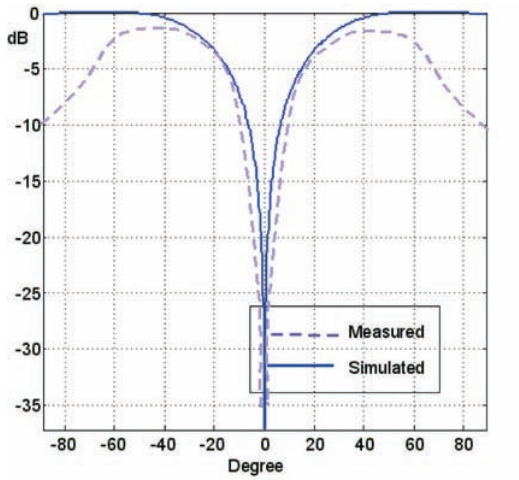

Fig. 10 Simulated and measured Radiation pattern in E and H plane (Mode 0).

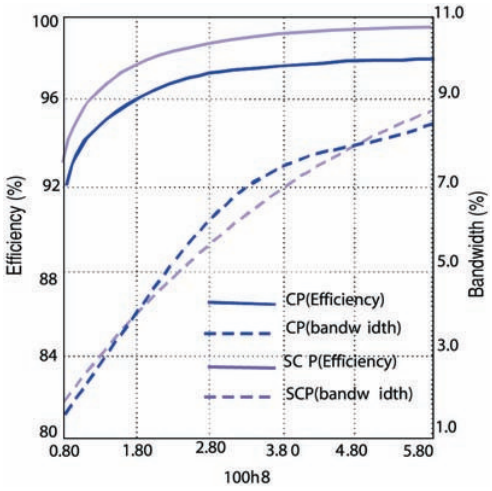

Fig. 11 Efficiency and Bandwidth versus thickness. CP(circular patch with b=28mm ε_r=2.5) and SCP(short circular patch with b=28mm a=19.3mm ε_r=2.5).

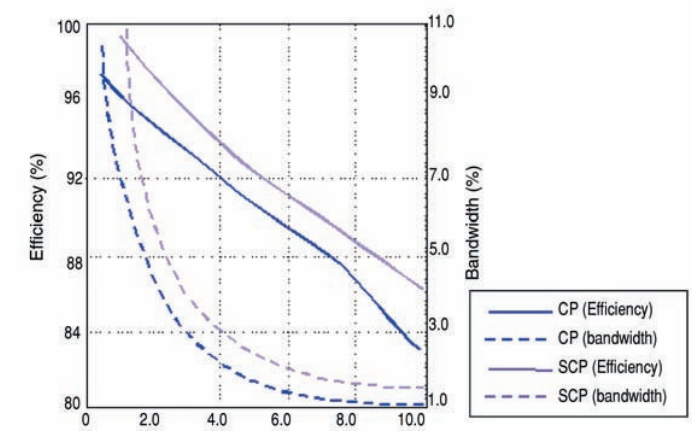

Fig. 12 Efficiency and Bandwidth versus permittivity. CP (circular patch with b=28mm h=1.58) and SCP (short circular patch with b=28mm a=19.3mm h=1.58).

Figures 11 and 12 represent the efficiency and bandwidth as a function of the thickness and the permittivity of substrate by circular patch (CP) and short circular patch (SCP).

As the radiating edge in this kind of patches is the outer bound, its radiation pattern is very similar to the corresponding one for the circular patch, but with a bigger efficiency. Besides, according to figure 1, note that the size of the short circuited patch can be modified in such a way that can be bigger than the corresponding circular patch. For that reason the radiating edge is bigger and its radiating performance is better than the conventional circular patch. It would also be possible to reduce the size of the short circuited patch by tuning externally the mode 0. This would yield a reduction in the size of the resonant patch what would reduce the antenna efficiency and gain getting a resonant structure that would hardly radiate.

A last comment can be made concerning the mode 0 for the conventional circular patch where this mode is a higher order one. In this case, the mode 0 does not present the quasi-static and tuning performance of the corresponding one in the short circuited patch. For that reason, the radiation pattern of the short circuited patch is less directive than the one for the circular patch. Besides, the lower the resonant frequency (for instance, by external tuning) the lower the directivity is.

CONCLUSIONS

The cavity model has been applied to analyze the short circuited ring antenna. This model has been applied to show the performance of the short circuited patch in front of the dielectric constant and its physical radius. Formulas for the resonant frequency, radiated field have been provided; an explicit expression for the input impedance has also been obtained and experimental results have been obtained. The accurate expressions for the radiation fields and an explicit formula for the input impedance constitute, from our point of view, new contributions to the study of short circuited patches.

One the major advantages of short circuited patch antenna is the possibility of constructing bigger resonant radiators than the conventional ones. For that reason, bigger efficiency and antenna gains can be achieved by properly choosing the resonant patch size. Other important characteristic is the fact that the fundamental mode is no longer TM_{11} (mode 1) but the TM_{01} which is the one that presents the lower cut-off frequency. This mode can be found in all the circular geometries but in the short circuited patch presents a quasi-static behavior that allows its tuning at a lower frequency than its natural resonant frequency.

REFERENCES

[1] R. Garg, P. Bhartia, I. Bahl, A. Ittipiboon. "Microstrip Antenna Design Handbook". Artech House, 2001.

[2] I.J. Bahl and P. Bhartia. "Microstrip Antennas", Artech House, Mass. 1980.

[3] M.D. Deshpande and M.C. Bailey. "Input Impedance of Microstrip Antenas", IEEE Trans. on Antennas and Prop, Vol. AP-30, no. 4, July 1982: 645-650.

[4] W.F. Richards, Y.T. Lo and D.D. Harrison. "An Improved Theory for Microstrip Antennas". IEEE Trans. MTT, 29 , no. 1, USA 1981: 38-46.

[5] Y. Lin and L. Shafai. "Properties of Centrally Shorted Circular Patch Microstrip Antennas", IEEE AP-S, Syracuse 1988: 700-703.

[6] Y. Lin and L. Shafai. "Characteristics of Concentrically Shorted Circular Patch Microstrip Antennas", IEE Proceedings, Vol. 137, no. 1, 1990: 18-24.

[7] Q. García. "Contribución al Estudio de las Antenas Autodiplexadas", Ph. Thesis, Chapter 3, Sevilla, May 1996.

[8] M.V. Schneider. "Microstrip Lines for Microwave Integrated Circuits", Bell Sist. Tech. Journal, USA 1969: 1421-1444.

[9] Y. S. Wu and F. J. Rosenbaum. "Mode Chart for Microstrip Ring Resonators". IEEE Trans. MTT, 21, USA 1973: 487-489.

[10] K.F. Lee and J.S. Dahele. "Characteristics of Annular Ring Microstrip Antenna", Electronic Letters, 1982, 28, no. 24-10: 1051-1052.

[11] Ch. Delaveaud, Ph. Leveque, B. Jecko. "New Kind of Microstrip Antenna: the Monopolar Wire-Patch Antenna", Electronic Letters, January 94: 1-2.